Carbohydrate Polymers 115 (2015) 325–333

Contents lists available at ScienceDirect

Carbohydrate Polymers

journal homepage: www.elsevier.com/locate/carbpol

Precise tailoring of tyramine-based hyaluronan hydrogel properties using DMTMM conjugation

Claudia Loebel[a,b,*], Matteo D'Este[a], Mauro Alini[a], Marcy Zenobi-Wong[b], David Eglin[a]

[a] AO Research Institute Davos, Davos Platz, Switzerland
[b] ETH Zurich, Cartilage Engineering+Regeneration, Department of Health, Science and Technology, Zürich, Switzerland

ARTICLE INFO

Article history:
Received 30 June 2014
Received in revised form 13 August 2014
Accepted 15 August 2014
Available online 15 September 2014

Keywords:
Hyaluronic acid
Tyramine
4-(4,6-Dimethoxy-1,3,5-triazin-2-yl)-4-methylmorpholinium chloride
Hydrogel

Chemical compounds studied in this article:
Hyaluronic acid sodium salt (PubChem CID: 23663392)
4-(4,6-Dimethoxy-1,3,5-triazin-2-yl)-4-methylmorpholinium chloride (DMTMM) (PubChem CID: 2734059)
Tyramine hydrochloride (PubChem CID: 66449)
N-(3-dimethylaminopropyl)-*N*′-ethylcarbodiimide hydrochloride (EDC) (PubChem CID: 2723939)
N-hydroxysuccinimide (NHS) (PubChem CID: 80170)

ABSTRACT

Injectable tyramine modified hyaluronic acid (HA–Tyr) hydrogels which are bio-orthogonally crosslinked with horseradish peroxidase (HRP) and hydrogen peroxide (H_2O_2) are excellent candidate biomaterials for drug delivery, regenerative medicine and tissue engineering. Ligation of tyramine to HA has been reported using the very well established *N*-(3-dimethylaminopropyl)-*N*′-ethylcarbodiimide hydrochloride (EDC) and *N*-hydroxysuccinimide (NHS) chemistry. Here we demonstrate the applicability of 4-(4,6-dimethoxy-1,3,5-triazin-2-yl)-4-methylmorpholinium chloride (DMTMM) as an alternative coupling agent to synthesize HA–Tyr conjugates. The optimized derivatization process allows accurate control of the degree of substituted Tyr on hyaluronan (DS_{mol}). Hence, viscoelastic properties, *in vitro* swelling and enzymatic digestion profiles of the crosslinked hydrogels can be precisely tuned *via* DS_{mol}. Our study demonstrates the advantages of DMTMM conjugation as a powerful tool to synthesize HA–Tyr hydrogels with properties exactly tailored for biomedical applications.

1. Introduction

Hydrogel-based biomaterials can mimic certain features of the extracellular matrix (ECM) of a tissue, provide an instructive three-dimensional (3D) microenvironment and serve as an effective delivery system for cell-based therapies (Slaughter, Khurshid, Fisher, Khademhosseini, & Peppas, 2009). Amongst the biopolymers serving as hydrogel backbone, hyaluronic acid (HA) plays a significant role in tissue development, but also in the biomedical field as one of the most commonly used biopolymers. It is ubiquitous, non-immunogenic, and a natural component of the extracellular matrix of various connective tissues with a key function in wound healing and the regeneration of these tissues (Fraser, Laurent, & Laurent, 1997). A major development in hydrogel-based technologies is the creation of an *in-situ* crosslinking mechanism which enables the system to be injectable, thus allowing an aqueous mixture of gel precursors and bioactive agents to be administered through a needle (Prestwich, 2011). In order to achieve the desired biomedical performance, hydrogels must display precise viscoelastic, swelling and degradation properties.

Recently, an injectable and biodegradable hydrogel system comprising hyaluronic acid–tyramine (HA–Tyr) conjugates has been reported for drug delivery and tissue engineering applications (Darr & Calabro, 2009; Lee, Chung, & Kurisawa, 2009; Toh, Lim, Kurisawa,

* Corresponding author at: AO Research Institute Davos, Clavadeler Strasse 8, 7270 Davos-Platz, Switzerland. Tel.: +41 81 414 25 49; fax: +41 81 414 22 88.
www.aofoundation.org/ari.
E-mail address: claudia.loebel@aofoundation.org (C. Loebel).

http://dx.doi.org/10.1016/j.carbpol.2014.08.097
0144-8617/

& Spector, 2012). HA–Tyr is enzymatically cross-linked to give a covalent network. The coupling is catalyzed by horseradish peroxidase (HRP) and uses hydrogen peroxide (H_2O_2) as oxidant. Unlike other methods of preparing HA-based hydrogels, a relatively low tyramine (Tyr) substitution is required to form stable constructs, leaving the majority of HA disaccharides unmodified. The crosslinking mechanism enables independent tuning of mechanical properties and gelation rate by varying the H_2O_2 and HRP concentration, respectively (Darr and Calabro, 2009; Lee et al., 2009; Toh et al., 2012). Additionally, crosslinking conditions are bio-orthogonal, *i.e.* mild, non-toxic and do not interfere with vital cellular processes. The formation of di-tyramine (di-Tyr) and di-tyrosine occurs under the influence of H_2O_2 and HRP (Gross & Sizer, 1959). Thus, Tyr-tyrosine bonds could be formed during *in vivo* crosslinking of the Tyr containing hydrogel onto the tyrosine-containing ECM proteins and provide improved tissue-hydrogel adhesion (Moreira Teixeira et al., 2012).

HA–Tyr synthesis has been reported using *N*-(3-dimethylaminopropyl)-*N*′-ethylcarbodiimide hydrochloride (EDC) and *N*-hydroxysuccinimide (NHS). Although very well established as method for HA conjugation, this carbodiimide chemistry has limitations. EDC acts as condensing agent, but if used alone it brings to the formation of an active intermediate which spontaneously rearranges to a non-reactive *O*-acyl isourea. This self-quenching can be avoided with the use of NHS, which forms a reactive NHS ester of HA reactive toward amines. NHS-activated HA displays maximum reactivity at pH 7–8 (URL, 2014). Unfortunately, Tyr is highly unstable at this pH. Moreover, formation of by-products has been observed (Darr and Calabro, 2009). Therefore it is not clear whether EDC/NHS can achieve the specific control of derivatization which is needed for the preparation of HA–Tyr derivatives suitable for biomedical applications. Similar to carbodiimides, 4-(4,6-dimethoxy-1,3,5-triazin-2-yl)-4-methylmorpholinium chloride (DMTMM) was initially developed for peptide synthesis. It has been shown that DMTMM is a very efficient agent for condensing a variety of carboxylic acids and amines (D'Este, Eglin, & Alini, 2014; Farkas & Bystricky, 2007; Farkas, Cizova, Bekesova, & Bystricky, 2013; Nimmo, Owen, & Shoichet, 2011). With these points in mind, we have investigated the use of DMTMM for the preparation of HA–Tyr hydrogels with precise rheological, swelling and degradation properties.

Since DMTMM is a relatively new method for HA conjugation and little is known about the stability of DMTMM in water we first investigated this aspect. Second, we optimized the reaction conditions through the variation of the stoichiometric ratios in order to obtain the most favorable conversion yield and desired substitution. The effect of temperature on the reaction kinetics was also investigated. Finally, we characterized the viscoelasticity, swelling behavior and degradation profile of hydrogels obtained from derivatives with different substitution.

2. Experimental

2.1. Materials

Hyaluronic acid sodium salt from *Streptococcus equi* (HANa) with weight-average molecular weight $Mw = 290$ kDa and polydispersion index $Mw/Mn = 1.86$, where Mn indicates the number-average molecular weight was purchased from Contipro Biotech s.r.o. (Czech Republic). 4-(4,6-Dimethoxy-1,3,5-triazin-2-yl)-4-methylmorpholinium chloride (DMTMM) from TDI (Zwijndrecht, Belgium). Hydrogen peroxide was purchased from LifeCore Biomedical (Chaska, MN, U.S.A.). Other chemicals were of analytical grade, purchased from Sigma Aldrich (Buchs, Switzerland) and used as received.

2.2. DMTMM stability in water

DMTMM stability was characterized using hydrogen-1 nuclear magnetic resonance (^{1}H NMR). Degradation of DMTMM was followed at 37 °C in deuterium oxide for up to 48 h. A series of ^{1}H-NMR spectra were acquired on a Bruker Avance AV-500 NMR spectrometer without residual HOD peak suppression. Percentage of degradation product was calculated by peak integration.

2.3. Synthesis and characterization of HA–Tyr conjugates

HA–Tyr was prepared by amidation of the carboxylic groups of HA with the amine groups of Tyr. Briefly, HANa (500 mg, 1.25 mmol carboxyl groups) was hydrated in 2-morpholinoethane sulfonic acid (MES) buffer (100 mM, pH 5.5, adjusted with NaOH 5 M) for 24 h at a final concentration of 1% (w/v). Subsequent to DMTMM, tyramine was added drop wise to the solution. The concentration of DMTMM and Tyr was varied to examine differences in Tyr substitution and hydrogel properties as a function of the molar ratio of Tyr, DMTMM and HA, respectively. This set of reactions was carried out at room temperature for 24 h, repeating each reaction twice. Coupling of HA–Tyr over time was studied at 24 °C (RT) or 37 °C under continuous stirring. Aliquots for precipitation were withdrawn after 2, 6, 10, 24, 48, 72, 96 and 120 h. Following enrichment of the solution with 8 vol% saturated sodium chloride; the product was precipitated using 96% ethanol. Several wash steps were subsequently performed and then the product was filtered and kept under vacuum for 48 h. The absence of chlorides in the final precipitate was assessed *via* Ag^+ assay. Finally, HA–Tyr was obtained as fine-grained white powder and stored at RT.

For comparison, HA–Tyr was synthesized *via* conventional carbodiimide chemistry (Darr and Calabro, 2009). Briefly, HANa (500 mg, 1.25 mmol carboxyl groups) was hydrated in MES Buffer (100 mM, pH 5.5, adjusted with NaOH 5 M) for 24 h at a final concentration of 1% (w/v). EDC and NHS (1/1 to HA) were added and kept stirring for 1 h at RT. Tyr (1/1 to HA) was dissolved in MES-buffer (100 mM, pH 5.5; 0.1% w/v) and added drop wise to the HA-solution. The reaction was maintained at RT for 24 h under continuous stirring. Products were either dialyzed (100 mM sodium chloride for 12 h and distilled water for additional 60 h) and lyophilized or precipitated as described above.

Synthesized HA–Tyr conjugates were characterized using UV–vis and ^{1}H NMR. UV spectra were recorded using a Multiskan™ GO Spectrophotometer in cuvette mode with 2 nm resolution. Molar degree of substitution (DS_{mol}, %) was calculated by measuring the Tyr absorbance at 275 nm of a 1 mg/ml HA–Tyr solution in ultrapure water. A calibration curve of Tyr in ultrapure water was used as a standard (Darr and Calabro, 2009). DS_{mol} is expressed as molar ratio of covalently bound Tyr residues to total carboxyl groups on HA. DS_{mol}, was further determined from ^{1}H NMR using deuterium oxide as solvent without residual HOD peak suppression. Spectra were calibrated using *N*-acetyl proton on glucosamine residue of HA as the chemical shift internal standard, and processed with Mestrenova software. DS_{mol} was determined by comparing the ratio of the areas under the aromatic peaks at 6.85 ppm 7.19/7.17 ppm and 7.38/7.36 ppm to the peak at 2.0 ppm (*N*-acetyl proton of HA).

2.4. Characterization of the hydrogels

2.4.1. Preparation of hydrogels

The synthesized conjugates with a concentration of 2.5% (w/w) were dissolved in 1 Unit/ml HRP (in PBS) overnight at 4 °C. Gelation was initiated by adding 0.34 mM H_2O_2 (in PBS) followed by gently mixing with a pipette tip. The above gelation protocol was optimized (optimization not shown here) while 0.34 mM H_2O_2 was

found to be the minimum concentration required to achieve proper gelation and was therefore used in all experiments. The H_2O_2 concentration of 0.34 mM is lower than other reported concentration for cells encapsulation (Lee, Chung, & Kurisawa, 2008).

2.4.2. Viscoelastic characterization

Rheological measurements were performed with an Anton-Paar rheometer equipped with a Peltier controller and plate-cone geometry, diameter 50 mm. The synthesized conjugates were hydrated in 1 Unit/ml HRP at 2.5% (w/w) overnight at 4 °C. Dissolved samples were mixed with 0.34 mM H_2O_2 directly on the bottom plate and the upper cone was lowered to a gap of 0.1 mm before gelation has been started. In order to allow a homogenous gelation process, hydrogels were allowed to cure for 30 min at 20 °C in the sample holder. A humid chamber was achieved by placing wet tissue paper around the platform and placing a chamber cover on top. The angular frequency sweep was conducted from 0.1 to 100 rad/s at 1% strain to determine the shear elastic modulus (G') and loss modulus (G'') of the hydrogels. The viscoelastic linear regime was determined and then mechanical spectra were carried out at 1% strain and 20 °C.

2.4.3. Equilibrium swelling

To examine the swelling properties, cross-linked hydrogel samples (200 μl) were prepared in cylindrical sample holders (diameter 8 mm) ($n = 3$). After incubation for 30 min at RT, samples were immersed in PBS (10 mM, pH 7.4) at 37 °C for 48 h until the swelling equilibrium had been reached. The swollen hydrogels were removed, carefully blotted to remove excess surface liquid, and the total swelled weight (W_S) was measured. The samples were lyophilized overnight and total dry weight (W_L) was measured. The swelling ratio was calculated using the following equation:

$$\text{swelling ratio} = \frac{W_S - W_L}{W_L}$$

2.4.4. Degradation assay

To determine the stability, we initiated cross-linking of the hydrogel samples (200 μl) in the sample holders as described above ($n = 3$) and allowed them to swell in PBS (10 mM, pH 7.4) for 24 h at 37 °C, after which the mass of the samples was measured (W_S). Degradation assay was performed using 10 Units/ml hyaluronidase in PBS (10 mM, pH 7.4) at 37 °C. At the chosen time points, hydrogels were removed, carefully blotted to remove excess surface liquid and the total weight (W_D) was measured. The percentage of hydrogel mass remaining in relation to the original swollen mass was calculated ($(W_D/W_S) \times 100$). Fresh buffer containing hyaluronidase was replaced at each time point. Hydrogels incubated in PBS without enzyme at 37 °C served as a control for the degradation profile.

3. Results and discussion

3.1. DMTMM stability in water

Use of DMTMM chloride in water solution as a coupling agent could potentially be limited by its instability. EDC, the most well-known water-soluble coupling agent has a half-life of 3.9 h in water at a pH of 5.0 (Gilles, Hudson, & Borders, 1990). DMTMM is stable in water at RT with no decomposition by demethylation or hydrolysis after 3 h (Kunishima et al., 1999; Raw, 2009). Little is known about later time points, and higher temperature. Therefore we investigated the stability of DMTMM in experimental conditions identical to those of the conjugation reactions. A series of ^{1}H-NMR spectra of DMTMM in deuterium oxide at 37 °C was recorded for up to 48 h.

The degradation of DMTMM in water can follow three main paths (Fig. 1A). In the first path, decomposition into 2-chloro-4,

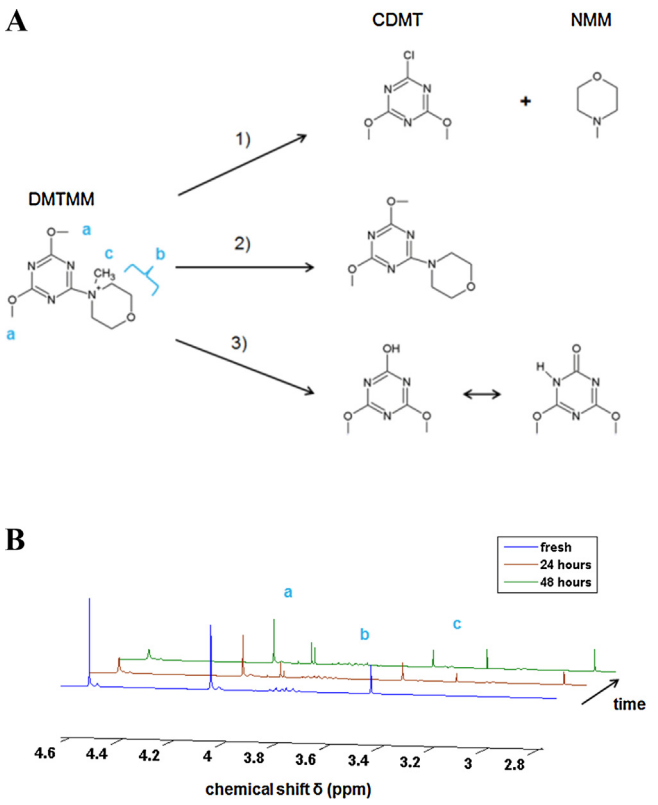

Fig. 1. DMTMM degradation: (A) main paths of DMTMM degradation: path (1) decomposition, path (2) demethylation and path (3) hydrolysis. (B) Representative series of ^{1}H-NMR spectra of DMTMM in deuterium oxide at 37 °C.

6-dimethoxy-1,3,5-triazine (CDMT) and *N*-methylmorpholine (NMM) takes place. This is the inverse of the preparation reaction commonly used for DMTMM (Kunishima et al., 1999). The CDMT generated is susceptible to further hydrolysis along a third path (Fig. 1A). In the second path, demethylation of the methyl group on the nitrogen of the morpholine ring occurs. In this case the triazine and morpholine rings are not split and a methanol molecule is released. In the third path, the triazine ring is hydrolyzed, resulting in 2,4-dimethoxy-6-hydroxy-1,3,5-triazine. This di-methyl ester of cyanuric acid gives keto-enol tautomerism. The compound can be originated directly from DMTMM, from CDMT generated as per path one or, presumably to a much lesser extent, from the demethylated species generated as per the second path.

^{1}H NMR spectrum of the freshly prepared DMTMM shows a sharp singlet at 4.17 ppm from the 6 methoxy protons (a); a sharp singlet at 3.56 ppm (c) from the methyl group bound to the nitrogen atom; a broad multiplet between 3.8 and 4.0 ppm from the protons in the NMM ring (b) (Fig. S1). At later time points spectrum evolves as follows (Fig. 1B). The sharp singlet at 4.17 ppm (a) decreases its relative intensity while other 3 sharp singlets at 4.06, 4.01 and 4.00 ppm appear over time. These peaks arise from the degradation products as per the 3 paths previously illustrated. The sharp singlet at 3.56 ppm (c) decreases its relative intensity while another singlet at 2.93 ppm develops, giving evidence of NMM formation as per path 1 and 3. The broad multiplet between 3.8 and 4.0 ppm (b) from the NMM methylene protons decreases its area and increases its complexity; at the same time a triplet of doublets at 3.2 ppm rises up. A sharp singlet at 3.34 ppm increases with the time, testifying methanol formation as per the second path. Another interesting feature is the broadening of the HOD peak at 4.64 ppm, attributed to the formation of more species with exchangeable protons. Such species include methanol, the di-methyl ester of cyanuric acid generated as per the third path and its tautomer.

Table 1
List of DS_{mol} for different samples showing the effect of DMTMM–Tyr ratio used for HA–Tyr synthesis after 24 h at RT (2 batches). Calculation is based on UV–vis analysis ($n = 3$) (see Section 2.2.1) and the conjugation was confirmed by ^{1}H NMR (see below).

HA–DMTMM–Tyr	DS_{mol} (%)
1–1–0.1	1.3 ± 0.2%
1–1–0.5	1.7 ± 0.2%
1–0.5–1	1.6 ± 0.2%
1–1–1	3.0 ± 0.5%
1–2–1	3.3 ± 0.3%
1–4–1	n.A.
EDC/NHS (1–1/1–1)	2.8 ± 0.3%

Interestingly, after 48 h 23% of DMTMM is demethylated as estimated from methanol protons signal integration. Likewise, from peak integration after 48 h 27% of the NMM methylene protons lie in the multiplet at 3.2 ppm rather than 3.9 ppm, attesting both first and second degradation path.

Degradation of DMTMM was also followed by UV–vis analysis. Since various species are involved in this process exact attribution of peak evolutions is not trivial (data not shown). The impact of DMTMM degradation on HA–Tyr coupling is discussed in the following paragraph.

3.2. Synthesis and optimization of HA–Tyr coupling

Table 1 lists the degree of substitution (DS_{mol}, %) obtained using different stoichiometric ratios of the reagents. To accomplish an exact comparison to conventional carbodiimide conjugation, final yields of conventional carbodiimide coupled HA–Tyr conjugates using a molar ratio of HA–EDC/NHS–Tyr (1–1/1–1) were analyzed. UV–vis absorbance measurements showed lower yields (DS_{mol} 2.79 ± 0.3%) obtained with EDC/NHS compared to DMTMM coupling (DS_{mol} 3.0 ± 0.5%) after 24 h at RT (Table 1).

The conjugation and DS_{mol} of HA–Tyr were confirmed by ^{1}H NMR analysis, which corresponds to the sum of components of the conjugate. The ligation does not give rise to any new resonance situated in a spectral region free of other signals, so conventional ^{1}H NMR spectroscopy cannot be used as direct proof of the chemical ligation. The observed gelation of the compounds is the proof that the ligation occurred. A comparison of the spectra for unsubstituted HA and HA–Tyr conjugates shows signals for the anomeric protons (ca. 4.5 ppm), sugar ring protons (four per monosaccharide between 3.2 and 4.0 ppm) and methyl protons of the *N*-acetyl group (3 per disaccharide, at 2 ppm) expected from both molecules (Fig. 2). The presence of Tyr in the product was verified by the resonances at 7.19–7.17 ppm (a) and 6.85 ppm (b) (Darr and Calabro, 2009). Semi-quantitative analysis of the DS_{mol} was performed by comparing the ratio of the areas under the aromatic peaks at 6.85 ppm, 7.19/7.17 ppm and 7.38/7.36 ppm to the peak at 2.0 ppm (*N*-acetyl glucosamine proton of HA).

Data in Table 1 show how different stoichiometric ratios of Tyr and DMTMM to HA can influence the DS_{mol}. Even using Tyr in amount as low as 10% in moles to HA a substitution of 1.3% was detected. Derivatization of this compound was confirmed by the gelation displayed (not shown). Usually, bioconjugations involving EDC/NHS use a large excess of ligand (Darr and Calabro, 2009; Kurisawa, Chung, Yang, Gao, & Uyama, 2005). Our result is a consequence of the increased efficiency of coupling of DMTMM compared to EDC/NHS. As a direct comparison, we performed the coupling reaction with both methods using stoichiometric amount of every reagent. Also in this case, DMTMM displayed higher coupling yield. The ratio Tyr–HA has a marked influence on the conjugation yield, and can be used to prepare conjugates with desired substitution. Conjugation yield increases also with increasing DMTMM–HA ratio. However when a ratio of 4–1 was used the obtained product was insoluble. Non-solubility was attributed to the higher amount of non-hydrophilic moieties bound to HA. Another possible reason is the modification of the pendant phenolic hydroxyl group on Tyr by the excess of DMTMM. The hypothesized adduct is illustrated in Fig. 2 (signal c) and is unique in DMTMM-mediated condensation of HA–Tyr. It should be noted that the same a/b and additional signal c can be seen whether Tyr is functionally bound or in a physical mixture with DMTMM. DMTMM is formed by the reaction of 2-chloro-4,6-dimethoxy-1,3,5-triazine (CDMT) with *N*-methylmorpholine (NMM). Therefore, reaction of CDMT directly with the hydroxyphenyl group on Tyr, whether free in solution or already covalently bound to HA through its amine group, forms Tyr-*O*-4,6-dimethoxy-1,3,5-triazine (Tyr-*O*-DMT) adducts on HA (Fig. 2, signal c). This assumption could be confirmed by decreasing the molar ratio of Tyr to DMTMM from 1 to 0.1 for the conjugation that results in a very low signal at 6.85 ppm (Table 1), but also increases the signal at 7.38/7.36 ppm.

Results were supported by UV–vis analysis of DMTMM–Tyr mixtures showing reduced absorbance at 275 nm when the molar ratio of Tyr to DMTMM was decreased (Fig. S2). It can therefore be assumed that Tyr-*O*-DMT adducts reduce the absorbance maximum of Tyr at 275 nm and are not functional in the crosslinking process. Noteworthy, it is essential to perform coupling reaction by premixing HA and DMTMM and add Tyr subsequently in order to minimize Tyr-*O*-DMT formation on HA.

On the basis of these results an equal molar ratio of DMTMM and Tyr to HA (1–1–1) results in low amounts of non-functional Tyr-*O*-DMT adducts while obtaining a high final yield (Table 1, Fig. S2).

DS_{mol} values obtained in the present study are slightly lower compared to previous studies (Darr and Calabro, 2009; Kurisawa et al., 2005). On the other hand the rheological profile of the obtained compounds is within the range of recently published HA–Tyr hydrogels (see below) (Lee et al., 2008). The presence of non-covalently bound Tyr might bias the values previously reported (Darr and Calabro, 2009; Kurisawa et al., 2005). It is further hypothesized that precipitation of the conjugates may be more efficient to avoid contamination of the final product with non-covalently bound Tyr. Indeed, after conjugation of HA–Tyr under same conditions (molar ratios of HA–DMTMM–Tyr of 1–1–1, RT, 24 h) dialyzed products (100 mM NaCl for 12 h followed by 60 h against distilled water), showed higher DS_{mol} of 5.0% for dialysis (Fig. S3) compared to a DS_{mol} value of 3.0% for precipitation (Table 1).

NaCl has been described as an important additive during early purification (dialysis) to avoid contamination with non-covalently bound Tyr molecules in the final product (Darr and Calabro, 2009). However, calculated DS_{mol} were still higher compared to precipitated samples. Noteworthy, mechanical properties of dialyzed conjugates were inferior compared to precipitated samples (data not shown). One explanation could be the formation of di-Tyr bonds between free Tyr molecules during cross-linking which inhibit the formation of stable di-Tyr bridges between covalently bound Tyr's on HA. In addition, precipitation as purification step for HA–Tyr conjugates is a clear advantage for scaling up, less expensive and much quicker compared to dialysis.

At neutral or alkaline pH Tyr is unstable, and therefore the conjugation has to be carried out at pH below 6. This condition hampers the use of EDC/NHS, which requires an acidic pH for the activation, but a slightly alkaline pH for the ligation step (Schante, Zuber, Herlin, & Vandamme, 2011). Moreover the fine pH tuning usually required for optimal EDC/NHS conjugation is not possible, making the accurate control of substitution degree difficult. DMTMM is a coupling agent less sensitive to pH, and therefore more appropriate for Tyr conjugation. The robustness of the process makes it more suitable for the chemical modification of carbohydrates with the

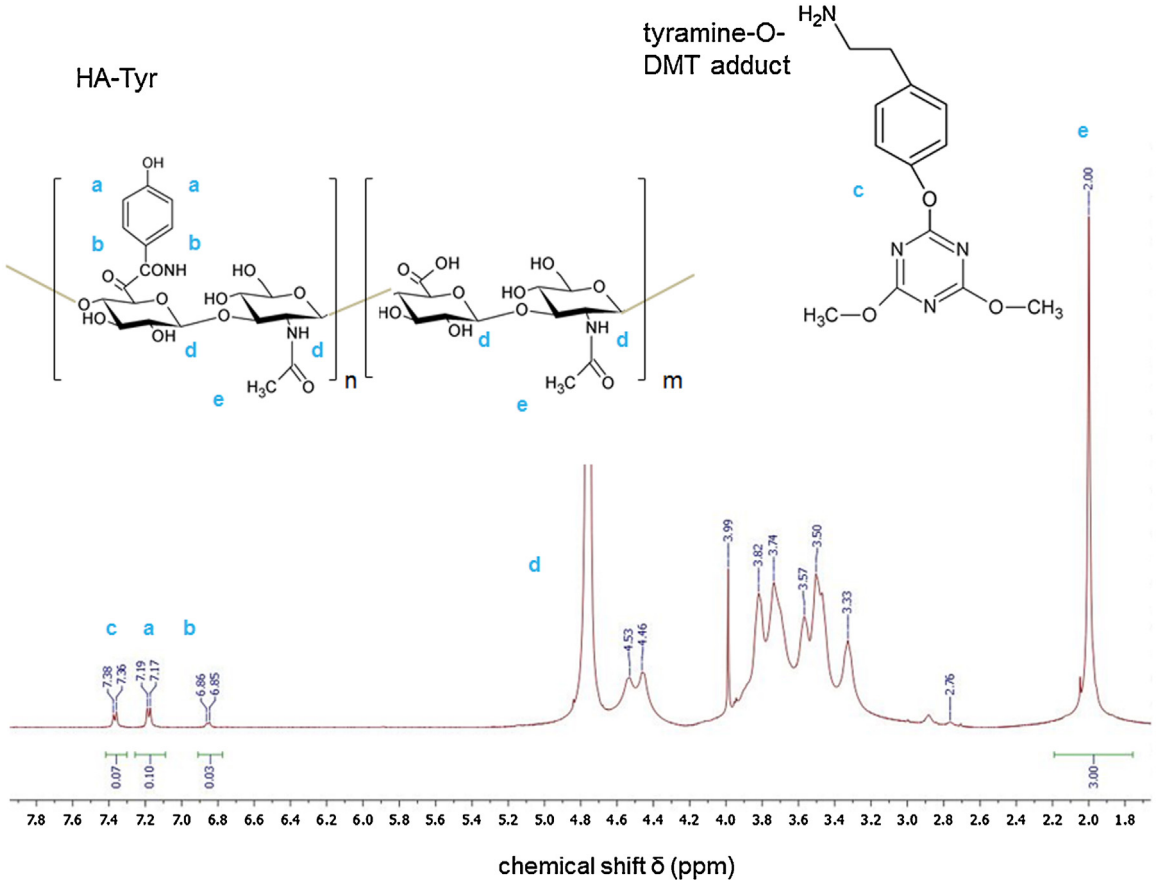

Fig. 2. ^{1}H NMR spectrum of the conjugate HA–Tyr.

degree of control needed for preparation of biomaterials and drug delivery systems.

3.3. HA–Tyr coupling kinetics and characterization

Coupling of HA–Tyr over time was studied at RT and 37 °C using equal molar ratios of DMTMM and Tyr over HA. In Fig. 3A the DS_{mol} is reported as a function of the reaction time. When the reaction is conducted at 37 °C the reaction kinetics is faster (Fig. 3A). The highest yield was obtained within 10 h (DS_{mol} 4.0 ± 0.1%) and HA–Tyr conjugates collected after 2 h at 37 °C (DS_{mol} 3.1 ± 0.11%) presented sufficient DS_{mol} for efficient cross-linking. Conjugation of HA–Tyr at RT required at least 48 h, reaching final yields of DS_{mol} 3.4 ± 0.15%. Once maximum yield was reached, DS_{mol} started to drop independent of final yield and reaction conditions (Fig. 3A).

Products isolated at different time points of reaction were analyzed by ^{1}H NMR in order to validate the use of absorbance at 275 nm for DS_{mol} quantification (Fig. 3B and Fig. S4). A correlation of DS_{mol} calculated from ^{1}H NMR and absorbance at 275 nm can be drawn (Fig. 3B). Noteworthy, HA–Tyr coupling at 37 °C did not show more impurities in ^{1}H NMR spectra than conjugates at RT.

The findings indicate that an increase of reaction temperature would be advisable for faster kinetics and higher yield. Usually, classical HA–Tyr conjugation is assumed to be completed after 24 h. To best of our knowledge, none of these studies reported comparing the DS_{mol} after earlier time points. It would be possible to further shorten time for HA–Tyr conjugation by increasing the

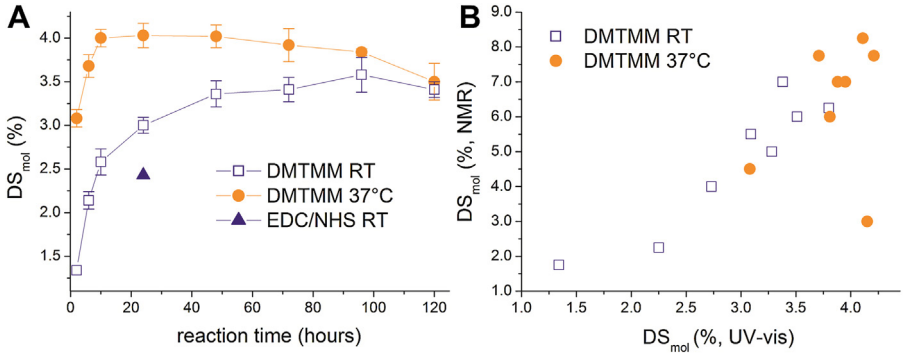

Fig. 3. (A) Kinetics of HA–Tyr conjugation for DMTMM conjugation performed at RT or 37 °C (2 batches) and EDC/NHS at RT for 24 h. DS_{mol} was analyzed with UV–vis using Tyr absorption maximum at 275 nm (n = 6). (B) Comparison of calculated DS_{mol} based on ^{1}H NMR spectra and absorbance at a peak maximum of 275 nm (Fig. S4).

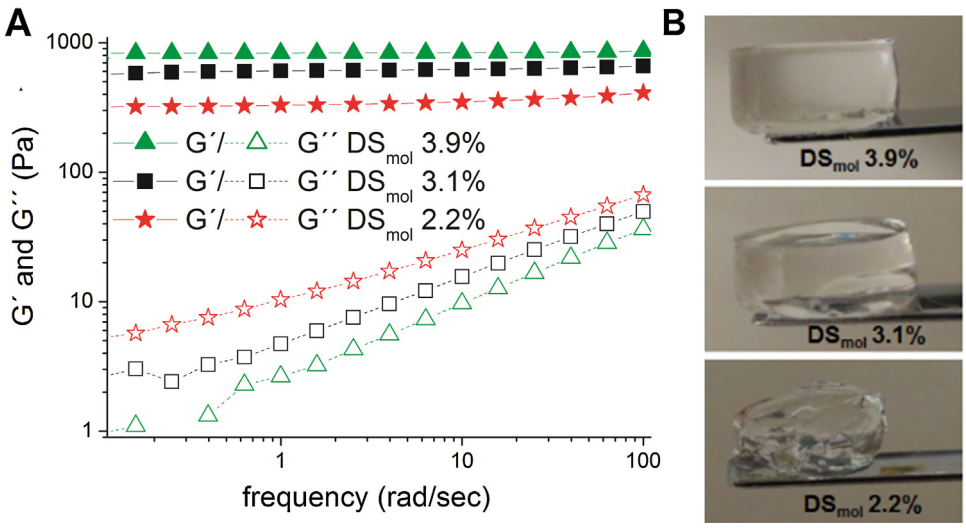

Fig. 4. (A) Rheological measurement (frequency sweep): Typical frequency dependence of the storage modulus G' and loss modulus G'' of HA–Tyr hydrogels and (B) images of the corresponding samples fabricated using 1 Unit/ml HRP and 0.34 mM of H_2O_2. Rheological measurement was taken with constant deformation of 1% (linear viscoelastic range) at RT.

reaction temperature (*e.g.* 60 °C). However, it has to be considered that HA is cleaved into low-molecular fragments at higher temperatures with undesired effects *in vitro* and/or *in vivo* (Stern, Asari, & Sugahara, 2006). Interestingly, lag time seems to be detrimental for final yields (Fig. 3A). After reaching the maximum levels of DS_{mol} either at RT or 37 °C, obtained yields dropped. Since the amount of Tyr-*O*-DMT adducts did not increase with time (Fig. 3B), chemical modifications of Tyr may cause a decrease in absorption at 275 nm (Fig. S2).

DS_{mol} calculated both by ^{1}H NMR and absorbance at 275 nm showed a good correlation (Fig. 3B). It is known that ^{1}H NMR is less accurate in determining low DS_{mol}. Since the signals of the Tyr-*O*-DMT adducts are included in the calculation of the final substituted Tyr, DS_{mol} values measured by ^{1}H NMR were overestimated compared to UV–vis calculations. However, a linear correlation of the DS_{mol} values, measured by ^{1}H NMR and UV–vis supports that the amount of non-functional adducts did not change with increasing yields of Tyr on HA (Fig. 3B). The results of ^{1}H NMR and UV–vis, together with the corresponding hydrogel properties confirm the functional Tyr substitution on HA and further validate the use of UV–vis absorbance measurement at 275 nm being a very sensitive probe to detect functional Tyr bound to HA.

Our findings further indicate that the HA–Tyr coupling kinetics and efficacy depend on the temperature and on the percentage of DMTMM remaining in solution upon degradation (Fig. 1). While DMTMM is more efficient and more reactive at 37 °C, it also decomposes quicker compared to RT.

3.4. Characterization of HA–Tyr hydrogels

3.4.1. Rheological properties

Cross-linking density is one of the key parameters in manipulating the mechanical properties of hydrogel systems. Variations in the gel precursor concentration, the molecular weight of the polymer, and the degree of conjugation of the cross-linking moiety are some of the common methods to control the cross-linking density (Baier, Bivens, Patrick, & Schmidt, 2003).

In the following experiments, concentrations of HA–Tyr (2.5% w/w), HRP (1 Unit/ml) and H_2O_2 (0.34 mM) were held constant and samples were incubated for 30 min prior to measurement. In order to assess the viscoelastic properties of cross-linked HA–Tyr, conjugates with different DS_{mol} were characterized by rheological studies using cone plate geometry at 20 °C. A typical frequency dependence of the storage modulus G' and loss modulus G'' of HA–Tyr hydrogels featured by different DS_{mol} are shown in Fig. 4A. For all specimens G' is markedly over G'' and almost independent of the frequency within the range analyzed, indicating a crosslinked network prior to analysis (Picout & Ross-Murphy, 2003). The graph also shows that at every frequency G'' follows an inverse order compared to G'.

Increasing the DS_{mol} clearly results in a denser network displayed by elevated G' values and the appearance of the fabricated hydrogels (Fig. 4B). Gelation times were unaffected by DS_{mol} with 300 ± 30 s (1 Unit/ml HRP/0.34 mM H_2O_2) and could be modified by the concentration of HRP (Lee et al., 2008). The fabricated HA–Tyr hydrogels are transparent and different DS_{mol} do not affect the transparency of the matrices (Fig. 4B). This feature is advantageous for analysis of encapsulated cells by microscopy.

A precise control over mechanical properties of hydrogels is an important tool for *in vitro* microenvironment studies of encapsulated cells. It is further essential to avoid any effects on cell viability and morphology. G' and G'' values at a frequency of 10 rad/s were chosen to illustrate the rheological properties of the HA–Tyr conjugates. As shown in Fig. 5, storage modulus G' at a frequency of 10 rad/s is correlated to DS_{mol} of HA–Tyr.

Accordingly, hydrogels with DS_{mol} of 1.3% were the weakest (G' value of 100 ± 35 Pa), whereas hydrogels with a DS_{mol} 3.9% showed the strongest G' values (875 ± 30 Pa) (Fig. 5). Control over DS_{mol} allows for predictive hydrogel properties as G' of the hydrogel matrices can reliably be predicted by the DS_{mol} of the HA–Tyr conjugates ($G' = 208 \times (DS_{mol}, \%) - 104$). The demonstrated control over the HA–Tyr hydrogels offers an extended range to tailor mechanical and physical properties.

As already described by earlier studies, there is a positive correlation between H_2O_2 concentration and storage modulus (Kurisawa, Lee, Wang, & Chung, 2010; Lee et al., 2008). In the enzymatic coupling reaction, HRP allows the formation of two Tyr radicals and two water molecules by reacting with one H_2O_2 molecule (Kurisawa et al., 2005). Consequently, the concentration of H_2O_2 would affect the number of Tyr cross-links and ultimately the mechanical strength of the hydrogel. Therefore it can be expected that different concentrations of H_2O_2 enable a further tuning of the mechanical properties (Fig. 6). To illustrate the effect of different H_2O_2 concentrations, three representative hydrogel

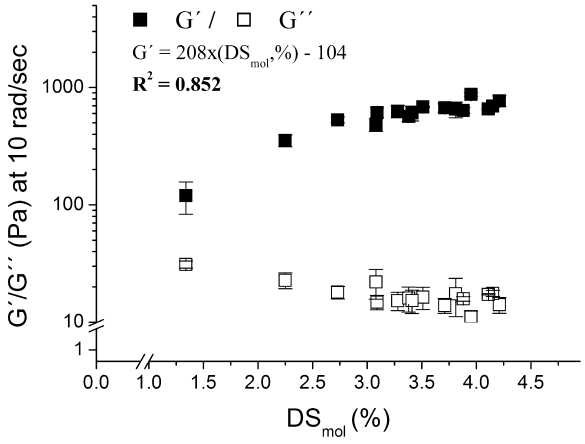

Fig. 5. Viscoelastic moduli at 10 rad/s as a function of the DS_{mol} in mol,% ($n = 3$): G' (filled symbols) with $R^2 = 0.852$ and G'' (empty symbols). Hydrogels were formed using 1 Unit/ml HRP and 0.34 mM H_2O_2 and incubated for 30 min prior to measurement.

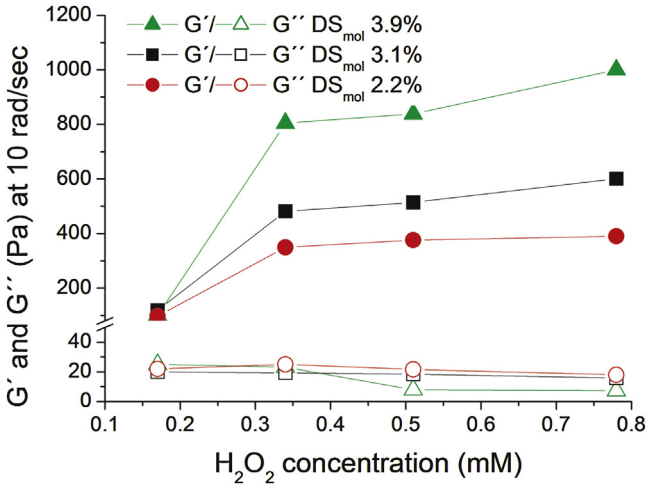

Fig. 6. Effect of H_2O_2 concentration on G' (filled shapes) and G'' (open shapes) for HA–Tyr hydrogels with DS_{mol} 3.9%, 3.1% and 2.2% respective.

matrices were chosen. Increasing the concentration of H_2O_2 results in higher mechanical strength (G') while the tendency was independent of the DS_{mol} (Fig. 6). However, an increase of storage modulus is accompanied with a change of loss modulus. While increased H_2O_2 concentrations induced an increase in G' at the expense of G'', tuning the DS_{mol} allow one to tune G' without affecting G'' (Fig. S5).

Noteworthy, after a certain threshold of H_2O_2 (>0.78 mM) the hydrogels become so brittle that rheology cannot be used any more. However, changing the concentration of H_2O_2 to vary stiffness and elasticity will invariably induce simultaneous changes in the cell response due to the effects of H_2O_2, making it difficult to interpret the contribution of various cues to an observed cellular response. To help elucidate the mechanism of cell-hydrogel interactions, it is highly desirable to develop biomimetic matrices that have independently tunable properties.

The HA–Tyr hydrogels reported here exhibit precisely tailored mechanical and morphological properties by adjusting the DS_{mol} without changes in H_2O_2 concentrations and the potential effects on cell behavior (Fig. 5). Since H_2O_2 concentrations are reported to dictate the amount of Tyr being involved in the effective formation of di-Tyr bonds, the matrix environment of encapsulated cells should not be affected. However, morphology and behavior of cells in hydrogel matrices with different degree of substituted Tyr have to be investigated. On the basis of an additional hydrogel matrix tuning through various H_2O_2 concentrations, DMTMM synthesized HA–Tyr conjugates can extend the range of viscoelastic and mechanical properties. It has been shown that the modulus of elasticity of the extracellular environment has profound effect on stem cell behavior (Engler, Sen, Sweeney, & Discher, 2006; Guvendiren & Burdick, 2013). The ability of cells to react to the mechanical properties of substrates is generally referred to as mechano-sensing and implies the action of the material on the cells and the action of the cell on the mechanical properties of the material (Vogel & Sheetz, 2006). The fabrication of HA–Tyr hydrogels with defined modulus of elasticity can be useful to study the interactions of cells with their biophysical microenvironment.

3.4.2. Swelling ratio

The swelling behavior of these hydrogels was probed gravimetrically by recording their water uptake over time until equilibrium. For all hydrogel formulations, the concentration of polymer (2.5% (w/w)), HRP (1 Unit/ml) and H_2O_2 (0.34 mM) were kept constant while the DS_{mol} ranged from 1.34% to 4.20% (Fig. 7A). All samples reached equilibrium after 48 h.

In general, an increase of DS_{mol} of bound Tyr to HA led to a linear decrease ($R^2 = 0.9259$) in the swelling capacity of the hydrogel (Fig. 7A). Hydrogels composed of HA–Tyr conjugates with the lowest DS_{mol} (1.3%) show by far the highest swelling ratio. In contrast, derivatives with DS_{mol} of 3.5–4.2% gained 10% less weight when

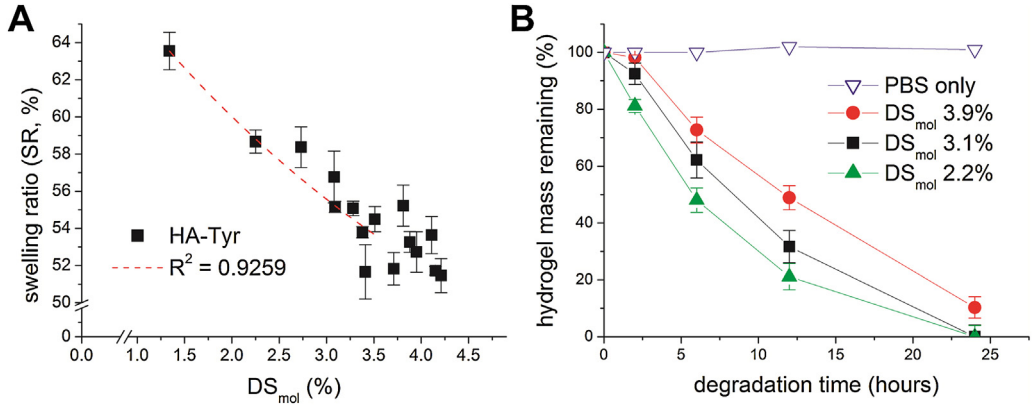

Fig. 7. Swelling and enzymatic digestion of cross-linked HA–Tyr: (A) swelling ratio (SR) for the samples as a function of the DS_{mol} ($n = 3$) ($R^2 = 0.9259$). Hydrogels were formed using 1 Unit/ml HRP and 0.34 mM H_2O_2 and incubated in PBS for 48 h at 37 °C to reach equilibrium ($n = 3$). (B) Enzymatic degradation of HA–Tyr hydrogels. Samples were allowed to pre-swell in PBS for 48 h at 37 °C. Open symbols: samples incubated in PBS only. Solid symbols: representative samples incubated in PBS containing 10 Units/ml hyaluronidase (average percentage of original weight ($n = 3$)). Results illustrate remaining hydrogel mass (%) of 3 representative samples over 24 h of degradation.

equilibrium was reached. The hydrogels with the highest swelling ratio, composed of HA–Tyr derivatives with DS_{mol} of 1.3%, are assumed to have a less cross-linked network. Likewise, the hydrogels with DS_{mol} 4.2% displayed the lowest swelling ratio, indicating that the swelling capacity was reduced due to more cross-links.

The hydrophilic/hydrophobic balance of the hydrogels and the degree of cross-linking are important parameters that control the equilibrium swelling and the dimensional change of the network. Swelling is not a continuous process and at the equilibrium, the elasticity of the network and the osmotic forces are balanced, there is no additional swelling (Ganji, Vasheghani-Farahani, & Vasheghani-Farahani, 2010). The cross-links act as tethering points between different HA chains of the hydrogel, preventing their movement away from each other. Other physicochemical cues further influence swelling ratio of hydrogels, in particular the porosity and pore size structure, which were not investigated in this study.

The excellent correlation of swelling ratio and DS_{mol} indicates that the control of DS_{mol} of DMTMM conjugated HA–Tyr constructs allows precise prediction of hydrogel swelling rate.

3.4.3. Degradation assay

The degradation of the HA–Tyr hydrogels was investigated by enzymatic digestion after adding hyaluronidase. HA is enzymatically degradable at its backbone which dependents on the availability of hyaluronidase and susceptibility of the modified hyaluronan to be cleaved by the enzyme.

To monitor how DS_{mol} affects degradation of the hydrogels *in vitro*, pre-swollen samples were incubated in PBS with 10 Units/ml hyaluronidase and PBS only (controls) at 37 °C. Their masses were recorded after 2, 6, 12, and 24 h (Fig. 7B).

After 24 h most of the hydrogels dissolved completely. Comparison of degradation kinetics with DS_{mol} showed hydrogels with low Tyr substitution (DS_{mol} 2.2%) degraded very fast and high DS_{mol} (DS_{mol} 3.9%) degraded more slowly (Fig. 7B). DS_{mol} 3.1% hydrogels displayed an intermediate degradation profile (Fig. 7B). Still, increasing the concentration of H_2O_2 would entail a denser network and therefore slow down degradation (Lee et al., 2008). These results suggest that the density of cross-links has an impact on the degradation process. No significant mass loss in the PBS control demonstrates that in these conditions the spontaneous degradation of hyaluronan is negligible at this pH and temperature.

It has been described earlier that hyaluronidase at low concentrations, as used in our study (10 Unit/ml), diffuse into the hydrogel network and hydrolyze HA not only from the surface but also through bulk erosion, causing a decrease in crosslinking density and loosening of the network (Lee et al., 2008). Accordingly, H_2O_2 concentrations of 0.32 mM may have diminished the effect of surface degradation. The lower crosslinking density of the hydrogels may allow faster diffusion of hyaluronidase into the hydrogel matrix, which is supported by the correlation of the degradation rates with DS_{mol}. Careful control of the hydrogel degradation rate is critical in tissue engineering application so that it can be matched to the growth rate of the new tissue (Nicodemus & Bryant, 2008) For hydrogel incorporated drugs or small molecules and their release, a precisely tailored degradation rate is indispensable. The conclusions are consistent with the viscoelastic features of the HA–Tyr hydrogels (Fig. 5).

4. Conclusion

In this paper we presented the use of DMTMM for the synthesis of HA–Tyr derivatives capable of *in situ* gelling within a biological environment. Major advantages of the hydrogel system are its injectability and adhesion to the tissue surface (Moreira Teixeira et al., 2012). The derivatization process was optimized studying the effect of different reagent feed ratios and operating temperatures. The process was further characterized by comparing the substitution efficiency with the degradation profile of the coupling agent. The study revealed the capability of this conjugation process to achieve an optimal control of the substitution degree, and the physical characteristics of the gel as a consequence. Specifically, swelling profile, *in vitro* enzymatic degradation and viscoelasticity were precisely tailored. The inherent advantages of DMTMM conjugation make this method a powerful tool for HA modification and for the preparation of semi-synthetic biomaterials in general. The obtained results encourage further studies exploring the use of DMTMM for polysaccharide modification and the preparation of biomaterials with properties exactly tailored toward drug delivery and tissue engineering applications.

Acknowledgments

The authors are grateful to Mrs. D. Sutter from ETH Zurich (Switzerland) for performing NMR analysis. The authors gratefully acknowledge the financial support from the SNF and the European Science Foundation, COST Action 1005 NAMABIO (grant number C11.0126).

Appendix A. Supplementary data

Supplementary data associated with this article can be found, in the online version, at http://dx.doi.org/10.1016/j.carbpol.2014.08.097.

References

Baier, L. J., Bivens, K. A., Patrick, C. W., Jr., & Schmidt, C. E. (2003). Photocrosslinked hyaluronic acid hydrogels: Natural, biodegradable tissue engineering scaffolds. *Biotechnology and Bioengineering*, *82*(5), 578–589.

Darr, A., & Calabro, A. (2009). Synthesis and characterization of tyramine-based hyaluronan hydrogels. *Journal of Materials Science: Materials in Medicine*, *20*(1), 33–44.

D'Este, M., Eglin, D., & Alini, M. (2014). A systematic analysis of DMTMM vs EDC/NHS for ligation of amines to hyaluronan in water. *Carbohydrate Polymers*, *108*, 239–246.

Engler, A. J., Sen, S., Sweeney, H. L., & Discher, D. E. (2006). Matrix elasticity directs stem cell lineage specification. *Cell*, *126*(4), 677–689.

Farkas, P., Cizova, A., Bekesova, S., & Bystricky, S. (2013). Comparison of EDC and DMTMM efficiency in glycoconjugate preparation. *International Journal of Biological Macromolecules*, *60*, 325–327.

Farkas, P., & Bystricky, S. (2007). Efficient activation of carboxyl polysaccharides for the preparation of conjugates. *Carbohydrate Polymers*, *68*(1), 187–190.

Fraser, J. R., Laurent, T. C., & Laurent, U. B. (1997). Hyaluronan: Its nature, distribution, functions and turnover. *Journal of Internal Medicine*, *242*(1), 27–33.

Ganji, F., Vasheghani-Farahani, S., & Vasheghani-Farahani, E. (2010). Theoretical description of hydrogel swelling: A review. *Iranian Polymer Journal*, *19*(5), 375–398.

Gilles, M. A., Hudson, A. Q., & Borders, C. L., Jr. (1990). Stability of water-soluble carbodiimides in aqueous solution. *Analytical Biochemistry*, *184*(2), 244–248.

Gross, A. J., & Sizer, I. W. (1959). The oxidation of tyramine, tyrosine, and related compounds by peroxidase. *The Journal of Biological Chemistry*, *234*(6), 1611–1614.

Guvendiren, M., & Burdick, J. A. (2013). Engineering synthetic hydrogel microenvironments to instruct stem cells. *Current Opinion in Biotechnology*, *24*(5), 841–846.

Kunishima, M., Kawachi, C., Monta, J., Terao, K., Iwasaki, F., & Tani, S. (1999). 4-(4,6-Dimethoxy-1,3,5-triazin-2-yl)-4-methyl-morpholinium chloride: An efficient condensing agent leading to the formation of amides and esters. *Tetrahedron*, *55*(46), 13159–13170.

Kurisawa, M., Chung, J. E., Yang, Y. Y., Gao, S. J., & Uyama, H. (2005). Injectable biodegradable hydrogels composed of hyaluronic acid–tyramine conjugates for drug delivery and tissue engineering. *Chemical Communications (Cambridge, England)*, *34*, 4312–4314.

Kurisawa, M., Lee, F., Wang, L. S., & Chung, J. E. (2010). Injectable enzymatically crosslinked hydrogel system with independent tuning of mechanical strength and gelation rate for drug delivery and tissue engineering. *Journal of Materials Chemistry*, *20*(26), 5371–5375.

Lee, F., Chung, J. E., & Kurisawa, M. (2008). An injectable enzymatically crosslinked hyaluronic acid–tyramine hydrogel system with independent tuning of mechanical strength and gelation rate. *Soft Matter*, *4*(4), 880–887.

Lee, F., Chung, J. E., & Kurisawa, M. (2009). An injectable hyaluronic acid–tyramine hydrogel system for protein delivery. *Journal of Controlled Release*, *134*(3), 186–193.

Moreira Teixeira, L. S., Bijl, S., Pully, V. V., Otto, C., Jin, R., Feijen, J., et al. (2012). Self-attaching and cell-attracting in-situ forming dextran–tyramine conjugates hydrogels for arthroscopic cartilage repair. *Biomaterials*, *33*(11), 3164–3174.

Nicodemus, G. D., & Bryant, S. J. (2008). Cell encapsulation in biodegradable hydrogels for tissue engineering applications. *Tissue Engineering, B: Reviews*, *14*(2), 149–165.

Nimmo, C. M., Owen, S. C., & Shoichet, M. S. (2011). Diels–Alder click cross-linked hyaluronic acid hydrogels for tissue engineering. *Biomacromolecules*, *12*(3), 824–830.

Picout, D. R., & Ross-Murphy, S. B. (2003). Rheology of biopolymer solutions and gels. *Scientific World Journal*, *3*, 105–121.

Prestwich, G. D. (2011). Hyaluronic acid-based clinical biomaterials derived for cell and molecule delivery in regenerative medicine. *Journal of Controlled Release*, *155*(2), 193–199.

Raw, S. A. (2009). An improved process for the synthesis of DMTMM-based coupling reagents. *Tetrahedron Letters*, *50*(8), 946–948.

Schante, C. E., Zuber, G., Herlin, C., & Vandamme, T. F. (2011). Chemical modifications of hyaluronic acid for the synthesis of derivatives for a broad range of biomedical applications. *Carbohydrate Polymers*, *85*(3), 469–489.

Slaughter, B. V., Khurshid, S. S., Fisher, O. Z., Khademhosseini, A., & Peppas, N. A. (2009). Hydrogels in regenerative medicine. *Advanced Materials*, *21*(32–33), 3307–3329.

Stern, R., Asari, A. A., & Sugahara, K. N. (2006). Hyaluronan fragments: An information-rich system. *European Journal of Cell Biology*, *85*(8), 699–715.

Toh, W. S., Lim, T. C., Kurisawa, M., & Spector, M. (2012). Modulation of mesenchymal stem cell chondrogenesis in a tunable hyaluronic acid hydrogel microenvironment. *Biomaterials*, *33*(15), 3835–3845.

URL. (2014). *Thermo Scientific EDC*. ⟨http://www.piercenet.com/instructions/2160475.pdf⟩

Vogel, V., & Sheetz, M. (2006). Local force and geometry sensing regulate cell functions. *Nature Reviews Molecular Cell Biology*, *7*(4), 265–275.